Cost vector analysis & multi-path entanglement routing in quantum networks

Hudson Leone,[1,2,*] Ashe Miller,[3,†] Deepesh Singh,[4] Nathan K. Langford,[1,2] and Peter P. Rohde[2,3,‡]
[1] *School of Mathematical and Physical Sciences, University of Technology Sydney, Ultimo, NSW 2007, Australia*
[2] *Centre for Quantum Software & Information (UTS:QSI), University of Technology Sydney, Ultimo, NSW 2007, Australia*
[3] *Hearne Institute for Theoretical Physics, Department of Physics & Astronomy, Louisiana State University, Baton Rouge LA, United States*
[4] *Centre for Quantum Computation & Communication Technology, School of Mathematics and Physics, The University of Queensland, St Lucia, Queensland 4072, Australia*

We present a static framework for analysing quantum routing protocols that we call the *cost-vector formalism*. Here, quantum networks are recast as multi-graphs where edges represent two-qubit entanglement resources that *could* exist under some sequence of operations. Each edge is weighted with a *transmission probability* that represents the likelihood of the pair existing and a *coherence probability* which is the likelihood that the pair is suitable for teleportation. Routing operations such as entanglement swapping and purification are then interpreted as *contractions on the multi-graph* with relatively simple rules for updating the edge-weights. Moreover, we extend our formalism to include routing scenarios over time by developing a compatible resource theory for quantum memories. We develop rudimentary greedy algorithms for routing in this framework and test them over a variety of toy networking scenarios. Our results indicate that congestion in quantum networks does not improve significantly when more nodes (computers) are added. Rather, we find that congestion is all but eliminated by waiting a small amount of time.

CONTENTS

* leoneht0@gmail.com
† ashemiller001@gmail.com
‡ dr.rohde@gmail.com; https://peterrohde.github.io/QuNet

I. INTRODUCTION

In classical networking, communication is carried out by transmitting bits of information encoded in an optical signal. Repeater stations amplify the signal at regular intervals which enables it to travel much further than it would be able to otherwise. Compare this with quantum networking, where the objective is to communicate quantum states that are typically encoded with one or more photons. General repeaters which "amplify" incoming states by duplicating them are impossible in quantum networking, since arbitrary copying of unknown quantum information is prohibited by the *no-cloning theorem*. This issue can be circumvented by instead distributing known entangled states between parties. Entangled states enable quantum information to be transmitted directly via *quantum state teleportation* (Bennett *et al.*, 1993) and, unlike the sensitive quantum data in a message, are fungible resources that can be refined with *entanglement purification* and extended over longer distances with *entanglement swapping*. These two actions (together with entanglement distribution), are the fundamental building blocks of *quantum communication protocols*, which are strategies for efficiently establishing entanglement links of arbitrary quality between parties in a quantum network.

A challenge of studying quantum communication protocols however is that they are *non-deterministic* and tend to have *many points of failure*. At any stage during routing, a key entanglement link could suddenly vanish and dramatically alter subsequent routing decisions. Naturally, the most effective way to benchmark quantum communication protocols is to simulate them directly (Coopmans *et al.*, 2020) (Dahlberg and Wehner, 2018) (Matsuo, 2019). Although this approach is accurate, it is likely to be computationally expensive for large networks with many competing end-users. In this paper, we propose a *static* framework for analysing quantum communication protocols that we call the *cost-vector formalism*. Our main insight is that quantum networks can be recast as multi-graphs where each link represents a partially entangled two-qubit state that *could exist* under some sequence of operations. Routing strategies in this framework are described as a sequence of contractions on the multi-graph that correspond to entanglement swapping and purification operations.

In the remainder of this section, we define quantum networking from first principles and introduce the problem of path-finding in quantum networks. Given the hardness of this subroutine, we identify two broad categories of path-finding heuristics. In section II we demonstrate how a simplified noise model allows us to find optimal paths in terms of a quantity called the *coherence probability*, which is the likelihood that a given pair is suitable for teleportation. Following this in section III, we formally introduce our cost-vector formalism. Each link of our network is weighted with two costs: a coherence probability p and a *transmission probability* (or *efficiency*) η which is the likelihood of the pair existing. We demonstrate how entanglement swapping and purification operations can be related to vertex and edge contractions of the multi-graph respectively (See Fig. 1). Consequently, we derive rules for updating the cost-vectors in either scenario. In section IV we extend our cost-vector formalism to include the use of quantum memories which enables us to consider entanglement routing over space and time. With the cost-vector formalism fully introduced, the latter part of the paper focuses on demonstrating some of its capabilities. We begin in section V by introducing some rudimentary multi-path routing algorithms, then we spend section VI testing them in a variety of networking scenarios.

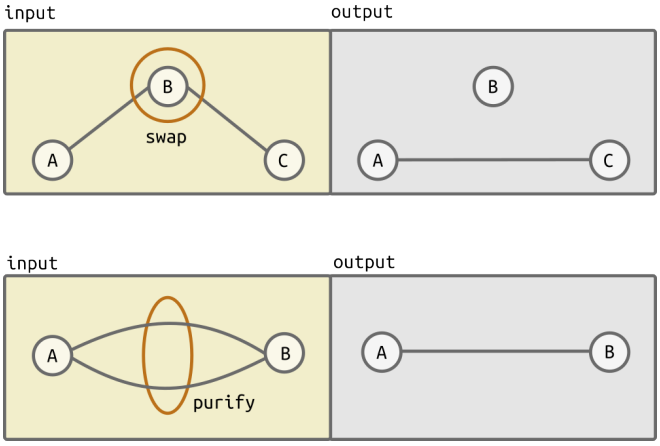

Figure 1: In the cost-vector formalism, the state of a network is represented with a multi-graph where edges are partially entangled two-qubit pairs that *could exist*. Top: Entanglement swapping between between edges (A, B) and (B, C) results in a link at (A, C). Bottom: A purification protocol reduces two edges in parallel to produce a *"higher quality"* link.

A. State teleportation and quantum networks

State teleportation is a well-established quantum communications protocol where one party transmits an arbitrary single qubit to another using a shared maximally entangled pair and a classical side channel. When the qubit being teleported is not a pure state, but is entangled with another qubit held by a third party, the entanglement is extended between the outer two qubits. This variant of state teleportation is called *entanglement swapping* (Pan *et al.*, 1998). Although there are inexhaustibly many types of entanglement, the scope of quantum networking is typically limited to the distribution of *two-qubit entanglement* to enable single qubit teleportation between end-users. No utility is lost in considering this restricted framework since arbitrarily large quantum states may be teleported across the network provided there are sufficiently many distributed entangled pairs.

Formally, a *quantum network* is a collection of quantum computers that are interconnected according to a graph of single qubit channels. These channels are completely positive maps on single qubit density operators that represent the error processes that occur as individual qubits are transmitted between computers, and they are ideally as close to the identity channel as possible. Equivalently, each link of the network may be represented as a completely positive and *trace-preserving* single qubit channel together with a transmission probability. Every computer in the network has the ability to generate entangled states, perform arbitrary local operations, store qubits in memory, measure states, and transmit qubits to adjacent quantum computers using the channels connecting them. We also assume that each computer is able to send messages to each-other with a *classical side channel*. Since there are infinitely many maximally entangled two qubit states, we assume by convention that the *target state* which the network aims to deliver is the maximally entangled pair $|\phi^+\rangle := \frac{1}{\sqrt{2}}(|00\rangle + |11\rangle)$. Without loss of generality then, the objective of a quantum network is to maximize the throughput of $|\phi^+\rangle$ states distributed between end-users. We note as well that $|\phi^+\rangle$ is one of the four *Bell pairs*:

$$\begin{aligned} |\phi^\pm\rangle &= \tfrac{1}{\sqrt{2}}(|00\rangle \pm |11\rangle) \\ |\psi^\pm\rangle &= \tfrac{1}{\sqrt{2}}(|01\rangle \pm |10\rangle) \end{aligned} \tag{1.1}$$

These states form a basis of the two qubit Hilbert space, and are each related to $|\phi^+\rangle$ by single qubit Pauli operations.

$$\begin{aligned} (I \otimes X)|\phi^+\rangle &= |\psi^+\rangle \\ (I \otimes Z)|\phi^+\rangle &= |\phi^-\rangle \\ (I \otimes XZ)|\phi^+\rangle &= |\psi^-\rangle \end{aligned} \tag{1.2}$$

Since any deviation from the target state $|\phi^+\rangle$ is treated as an error, this leads to the interpretation that $|\phi^-\rangle, |\psi^+\rangle$, and $|\psi^-\rangle$ are maximally entangled pairs that have suffered a phase-flip error, a bit-flip error or both respectively on one of their qubits (note that because of the states' symmetry, it doesn't matter which qubit suffered the error).

1. Fidelity as a threshold for error tolerance

In practice, distributing $|\phi^+\rangle$ states between end-users is impossible, not only because of the noisy channels connecting them and the asymptotic nature of practical purification protocols, but also because of the device level noise that caps the accuracy states can be purified to. We must therefore refine our objective by insisting that distributed states are close approximations of $|\phi^+\rangle$. Formalising the notion of "approximate" requires the specification of a *distance measure* between states (Gilchrist *et al.*, 2005), the most common choice being the *state fidelity*. In general, the fidelity between two states is defined

$$F(\rho, \sigma) = \mathrm{Tr}(\sqrt{\sqrt{\rho}\sigma\sqrt{\rho}}) \tag{1.3}$$

However since our comparison state $|\phi^+\rangle$ is pure, the fidelity simplifies to,

$$F(\rho, |\phi^+\rangle) = \langle\phi^+|\rho|\phi^+\rangle \tag{1.4}$$

In this special case, the fidelity is interpreted as the probability that a projective measurement on the imperfect pair will collapse it to the $|\phi^+\rangle$ state. Notably, pair fidelity can also be related to the *maximum teleportation fidelity* $F_{\max}$, which is the highest attainable qubit fidelity when using the pair ρ for state teleportation (Horodecki *et al.*, 1999).

$$F_{\max} = \frac{2F + 1}{3} \tag{1.5}$$

We now amend our definition of the quantum network by clarifying that it must deliver states ρ_{ϕ^+} that are ϵ-*close* with respect to $|\phi^+\rangle$ in fidelity, which is to say

$$1 - F(\rho_{\phi^+}, |\phi^+\rangle) \leq \epsilon \quad \epsilon \ll 1 \tag{1.6}$$

2. Swapping vs. distribution

One subtlety of quantum networking that must be addressed is that there are *two ways* of propagating entanglement through the network. Entanglement may be either *distributed* between nodes by forwarding entangled qubits to neighboring computers, or it may be extended by performing *entanglement swapping* on two "adjacent" pairs. As a rule, it is never beneficial to distribute entanglement beyond one's nearest neighbor since repeated transmissions suffer considerably more loss than swapping along the path.

We can demonstrate this claim with a simple thought experiment: Suppose that two parties Alice and Bob want to share entangled pairs but are separated by n consecutive channels each with transmission probability p_t. They have the option of either transmitting their pairs directly or coordinating the network to distribute and swap entanglement at each step. Let us assume that each swapping operation succeeds with probability p_s. If Alice and Bob attempt direct transmission, their success probability is p_t^n. On the other hand if they distribute and swap, the

probability is $np_T p_s^{(n-1)}$. Since p_s is justifiably assumed to be much higher than p_t, we see that $np_t p_s^{(n-1)} \gg p_t^n$ holds for all $n \geq 2$. Consequently, we see that it is never advantageous to distribute entanglement beyond one's nearest neighbor.

B. Two path-finding paradigms in quantum networking

In any networking scenario, we are frequently interested in *optimal path finding* which, in our context, means finding the sequence of channels that maximizes the rate that ρ_{ϕ^+} states are distributed between a given pair of end-users. Here, we preface our discussion on this topic by drawing an important distinction between *path finding* and *entanglement routing*, where we take the latter term to mean finding the optimal entanglement distribution strategy *given* a particular path in the network. In general, the throughput of a routing protocol depends both on the order of entanglement swappings (Chang and Xue, 2022) and the order of purifications (Goodenough *et al.*, 2021). Although there are exponentially many valid routing protocols, semi-definite programs exist that efficiently find orderings with near optimal throughput (Jiang *et al.*, 2007) (Goodenough *et al.*, 2021). Although these techniques simplify things considerably by allowing network engineers to explicitly compare the performance of paths, the fact remains that finding the optimal path is a highly non-trivial problem. The objective then for quantum path-finding is to identify the *most-promising* path(s) in the network according to some heuristic for the semi-definite programs to evaluate. This is done by associating each network channel with an additive scalar cost and using a path-finding algorithm on the resulting weighted graph. If the heuristic chosen is well-motivated, we can be fairly confident that the shortest path with respect to that heuristic will have a routing strategy close to the global optimum.

How then do we develop a good heuristic? Broadly speaking, the answer is to make approximations about the network and the actions we can perform on the network until there is sufficient granularity to describe processes without having to worry about the overwhelming variety of things that can occur. In the former category, we simplify the network picture by treating optimal path finding under the assumption that every channel is trace-preserving. If we allowed ourselves to consider photon loss in addition to channel effects, we would end up with an instance of multi-objective path finding, which is a well known hard problem (Zajac and Huber, 2021). This is not to say that loss is irrelevant however! Clearly channel loss is a critically important factor in entanglement throughput. Later, we will show how loss is incorporated into the *cost-vector* framework we are building towards. In the latter of the aforementioned categories, we simplify the operations we can perform on the network by restricting ourselves to one of *two heuristic paradigms* that are based on opposite-extreme purification strategies. In the *link-level paradigm*, we require that all entanglement is purified to ρ_{ϕ^+} before any swapping takes place. In the *end-level paradigm*, we prioritise swapping and defer all purification to the end-users. The utility of limiting our attention to these two scenarios is that any purification strategy is, in some sense, *between* these two edge-cases. It may advantageous then to analyse network paths using one heuristic from each paradigm in order to get a sense of what the entanglement throughput might be for a more generic routing algorithm.

Having motivated the two paradigms, let us now examine the major advantages and disadvantages of each. The main advantage of the link-level paradigm is that it offers a meaningful routing heuristic that is easy to calculate: Let the weight of each channel be the average number of channel calls needed to produce an ideal pair over that link. This quantity can be calculated using techniques from channel coding theory. Finding the optimal path with respect to this heuristic is therefore equivalent to finding the path with the fewest number of total expected calls required to establish end-to-end entanglement. The main disadvantage of the link-level paradigm is that its routing algorithms have comparatively high latency. This is because each entanglement link can only be established after a successful purification is performed. If the quantum memories available at each computer are weak, networking in this regime may prove challenging as decoherence builds during the dead time needed to establish every link in the path. On the other hand, we expect that the latency is minimized in the end-level paradigm since the only precondition for swapping is whether or not the raw resources exist between links. The trade-off for this paradigm however, is that it is difficult to find a heuristic that accurately encapsulates all facets of the optimization problem. Di Franco and Ballester demonstrated this difficulty by showing that optimal lossless path finding with respect to *entanglement negativity* could, in the special case where each channel is diagonal (Arab, 2021), be re-framed as an instance of multi-objective path-finding which we have already established is a hard problem. Developing a heuristic for this scenario therefore requires insight into how these competing objectives ought to be balanced. Since this is knowledge we do not claim to possess, we opt for a more general approach where we simplify the description of channel noise in such a way that it becomes possible to perform lossless path-finding with respect to a single cost.

II. OPTIMAL PATH-FINDING WITH COHERENCE PROBABILITY

In the previous section, we made the argument that optimal path-finding in the end-level paradigm is a hard

problem, even in the simplified case of diagonal-noise where each channel has some probability of applying any of the three single qubit Pauli errors. Here, we show how further constraining our noise model to *partially-depolarizing* or *partially-dephasing* error channels allows us to develop a path-finding heuristic over a single cost. We begin this section with some definitions before moving onto our main observation that entanglement swapping preserves the structure of partially depolarized and partially dephased states. We conclude by demonstrating how this property can be used to specify a single cost heuristic for these noise models and showing how this cost can be related to the fidelity with respect to $|\phi^+\rangle$.

A. Definitions

Definition 1. *A **partially depolarizing channel** $\mathcal{E}_d(p,\hat{\rho})$ is a single qubit channel with the action*

$$\mathcal{E}_d(p,\hat{\rho}) = p\hat{\rho} + (1-p)\frac{1}{2}I \tag{2.1}$$

The interpretation of this channel is that the input state passes through as intended with probability p or else is mapped to the maximally mixed state with probability $1-p$.

Definition 2. *The **partially depolarized pair** Δ_p is a two qubit mixed state of the following form*

$$\Delta_p = p|\phi^+\rangle\langle\phi^+| + (1-p)\frac{1}{4}I \tag{2.2}$$

Observe that Δ_p is the state that results from sending one qubit of a maximally entangled pair through a partially depolarizing channel with success probability p.

$$\Delta_p = \mathcal{E}_{\mathrm{d}}(p, |\phi^+\rangle\langle\phi^+|) \tag{2.3}$$

Because of this correspondence, we will refer to p as the *coherence probability* of the state. The definitions for the partially dephasing channel and the partially dephased pair are similar and thus will be treated in brief detail.

Definition 3. *A **partially dephasing channel** $\mathcal{E}_{\sigma_i}(p,\hat{\rho})$ is a single qubit channel with the action*

$$\mathcal{E}_{\sigma_i}(p,\hat{\rho}) = p\hat{\rho} + (1-p)\ \sigma_i\hat{\rho}\sigma_i \tag{2.4}$$

Where $\sigma_i \in \{X,Y,Z\}$

Definition 4. *A **partially dephased pair** $\delta_p^{\sigma_i}$ in the σ_i direction (where $\sigma_i \in \{X,Y,Z\}$) is a two qubit mixed state of the form*

$$\delta_p^{\sigma_i} = p|\phi^+\rangle\langle\phi^+| + (1-F)(I\otimes\sigma_i)|\phi^+\rangle\langle\phi^+|(I\otimes\sigma_i) \tag{2.5}$$

As with partially depolarized states, we also have that,

$$\delta_p^{\sigma_i} = \mathcal{E}_{\sigma_i}(p, |\phi^+\rangle\langle\phi^+|) \tag{2.6}$$

Finally, we conclude this section of definitions by defining a term that encompasses our restricted error model.

Definition 5. *In the **decoherence model of quantum networking**, either all network channels are partially depolarizing channels, or all channels are partially dephasing channels.*

B. Swapping on partially depolarized and partially dephased pairs

In this section, we demonstrate that entanglement swapping between two states in the decoherence model of networking with coherence probabilities p_1 and p_2 respectively results in another partially depolarized state with coherence probability p_1p_2.

Definition 6. *Let $\rho_{1,2}$ and $\sigma_{3,4}$ be two-qubit density operators with subscripts denoting qubit labels. The entanglement swapping operation $\mathcal{E}_{\mathrm{swap}}$ on these states is defined*

$$\mathcal{E}_{\mathrm{swap}}(\rho\otimes\sigma) = \frac{\langle\phi^+|_{2,3}(\rho_{1,2}\otimes\sigma_{3,4})|\phi^+\rangle_{2,3}}{\mathrm{Tr}(\langle\phi^+|_{2,3}(\rho_{1,2}\otimes\sigma_{3,4})|\phi^+\rangle_{2,3})} \tag{2.7}$$

Where $|\phi^+\rangle_{2,3}$ is short-hand for the projection $I_1\otimes|\phi^+\rangle_{2,3}\otimes I_4$

In principle, entanglement swapping will not always result in a projection of $|\phi^+_{2,3}\rangle$ but can include projections onto the other three Bell states as well. These other three scenarios are detectable and correctable with local operations, and so are not formally incorperated in our definition of swapping.

Theorem 1. *Let Δ_{p_1} and Δ_{p_2} be two partially-depolarized entangled pairs of coherence probabilities p_1 and p_2 respectively. An entanglement swapping operation on these states results in another partially depolarized state with coherence probability p_1p_2.*

Proof. By definition,

$$\begin{aligned}\Delta_{p_1} &= p_1|\phi^+\rangle\langle\phi^+| + (1-p_1)\tfrac{1}{4}I\\ \Delta_{p_2} &= p_2|\phi^+\rangle\langle\phi^+| + (1-p_2)\tfrac{1}{4}I\end{aligned} \tag{2.8}$$

Using the shorthand $[\phi^+] := |\phi^+\rangle\langle\phi^+|$:

$$\begin{aligned}&\mathcal{E}_{\mathrm{swap}}(\rho_1\otimes\rho_2) = p_1p_2\ \mathcal{E}_{\mathrm{swap}}([\phi^+]\otimes[\phi^+])\\ &+ p_1(1-p_2)\ ([\phi^+]\otimes\frac{1}{4}I) + (1-p_1)p_2\ \mathcal{E}_{\mathrm{swap}}(\frac{1}{4}I\otimes[\phi^+])\\ &+ (1-p_1)(1-p_2)\ \mathcal{E}_{\mathrm{swap}}(\frac{1}{4}I\otimes\frac{1}{4}I)\end{aligned} \tag{2.9}$$

Evidently $\mathcal{E}_{\text{swap}}([\phi^+]\otimes[\phi^+]) = [\phi^+]_{1,4}$, and it is straightforward to verify that the other three terms are maximally mixed states. The resulting state is therefore

$$\mathcal{E}_{\text{swap}}(\Delta_{p_1} \otimes \Delta_{p_2}) = p_1 p_2 [\phi^+] + (1 - p_1 p_2)\frac{1}{4} I \quad (2.10)$$

Which, as asserted earlier, is a partially depolarized pair with coherence probability $p_1 p_2$.

□

It is similarly straightforward to show that if $\delta_{F_1}^{\sigma_i}$ and $\delta_{F_2}^{\sigma_i}$ are partially dephased pairs with respect to σ_i, a swapping operation on these two states will result in a partially dephased pair with coherence probability p_1, p_2. We omit this proof for brevity and, as a rule, tend to omit proofs for all scenarios involving partially-dephased states since they are virtually identical.

Corollary 1. *The entanglement swapping operation on partially depolarized states is* ***associative****, meaning that for three partially dephased states $\Delta_{p_1}, \Delta_{p_2}, \Delta_{p_3}$ we have that,*

$$\mathcal{E}_{swap}(\mathcal{E}_{swap}(\Delta_{p_1}, \Delta_{p_2}), \Delta_{p_3})) = \mathcal{E}_{swap}(\Delta_{p_1}, \mathcal{E}_{swap}(\Delta_{p_2}, \Delta_{p_3})) \quad (2.11)$$

Proof. From theorem 1, we know that a swapping operation on partially depolarized pairs with coherence probabilities p_1, p_2 results in a partially depolarized pair with coherence probability $p_1 p_2$. It follows immediately from the associative property of integer multiplication that entanglement swapping on these states is also then associative. □

C. An additive path-finding cost

Having established the fact that swapping operations are essentially multiplicative on the coherence probabilities of partially depolarized and partially dephased states, we are now in a position to consider what the overall coherence probability is when routing over an an arbitrary network path. We recall from our discussion in sec. I.A.2 that the first step in any routing protocol is to distribute entanglement between each pair of nodes. Assuming hypothetically that all pairs arrive at their destinations, the coherence probability of a state swapped through a network path is given by the following theorem.

Theorem 2. *Let $\mathcal{E}_d(p_1), \mathcal{E}_d(p_2), \cdots, \mathcal{E}(p_n)$ be a path in a quantum network connecting two end-users. The coherence probability of the path is*

$$P_{path} = p_1 \times p_2 \times \cdots \times p_n \quad (2.12)$$

Proof. We begin our routing protocol by assuming that entangled pairs are distributed between each link in the path. The initial state of the system is therefore

$$\Delta_{p_1} \otimes \Delta_{p_2} \otimes \cdots \otimes \Delta_{p_n} \quad (2.13)$$

By corollary 1 we know that entanglement swapping is associative over partially depolarized states. Applying swapping on the terms from left to right

$$\mathcal{E}_{\text{swap}} \cdots \mathcal{E}_{\text{swap}}(\mathcal{E}_{\text{swap}}(\Delta_{p_1} \otimes \Delta_{p_2}), \Delta_{p_3}), \cdots \Delta_{p_n}) \quad (2.14)$$

And this is easily seen by inspection to produce the state $\Delta_{P_{path}}$ between the end-users.

□

Theorem 2 tells us that the coherence probability of a pair swapped through a path is the product of the coherence probabilities of the constituent links. Finding the optimal path in terms of the coherence probability is therefore equivalent to finding the path whose links multiply to give the highest overall success probability. Optimal path-finding algorithms however require *additive* (not multiplicative) costs. To develop an additive cost over success probabilities we observe that,

$$\prod_{i=1}^{n} p_i = \sum_{i=1}^{n} \log(p_i) \quad (2.15)$$

Which indicates that coherence probabilities can be converted into an additive cost by taking the logarithm of each term. Notice however that $\log(p_i) \leq 0$ since $0 < p_i \leq 1$. Since path-finding algorithms require (by convention) the shortest path to have the smallest overall cost, we require a sign flip on each term. The additive cost with respect to the coherence probability is therefore

$$c_i = -\log(p_i) \quad (2.16)$$

D. Relating coherence probability with state fidelity

In this section we show how, using basic algebra, the coherence probabilities of partially depolarized and partially dephased pairs are related to the fidelity with respect to the maximally entangled state $|\phi^+\rangle\langle\phi^+|$.

Theorem 3.

$$F(\Delta_p, |\phi^+\rangle\langle\phi^+|) = \frac{1 + 3p}{4} \quad (2.17)$$

Proof.

$$\begin{aligned}\Delta_p &= p|\phi^+\rangle\langle\phi^+| + (1-p)\frac{1}{4}I \\ &= p[\phi^+] + (1-p)\frac{1}{4}([\phi^+] + [\phi^-] + [\psi^+] + [\psi^-]) \\ &= \frac{1+3p}{4}[\phi^+] + (1-p)\frac{1}{4}([\phi^-] + [\psi^+] + [\psi^-])\end{aligned} \tag{2.18}$$

And since $[\phi^+]$ is orthogonal to the other three Bell pairs the fidelity of this state with respect to $[\phi^+]$ is $(1+3p)/4$ as required. □

Theorem 4.

$$F(\delta_p^{\sigma_i}, |\phi^+\rangle\langle\phi^+|) = \frac{1+p}{2} \tag{2.19}$$

Proof.

$$\begin{aligned}\delta_p^{\sigma_i} &= p[\phi^+] + (1-p)\frac{1}{2}\Big([\phi^+] + (I\otimes\sigma_i)[\phi^+](I\otimes\sigma_i)\Big) \\ &= \frac{1+p}{2}[\phi^+] + (1-p)\frac{1}{2}(I\otimes\sigma_i)[\phi^+](I\otimes\sigma_i)\end{aligned} \tag{2.20}$$

Similar to the previous theorem, the first term is the only element that contributes, giving us an overall fidelity of $(1+p)/2$ as required. □

III. THE COST-VECTOR FORMALISM

Non-determinism is a pervasive fact of quantum networking. Entangled photons can be lost in transmission, entanglement swapping between photons has a maximum success rate of 50% (Pan *et al.*, 1998), and entanglement purification is inherently probabilistic. The consequence of this non-determinism is that entanglement routing is a *highly volatile* process with many points of failure. Although the performance of routing protocols can be gauged by simulating the network, this may prove costly for large networks with many competing end-users. Here, we present an alternative *static* picture of quantum networking that we call the *cost-vector formalism*. At the core of this formalism is the insight that every pair that *could* exist in the network (by following some sequence of swapping and purification operations) can be characterised with a *transmission probability* (*or efficiency*) η and a *coherence probability* p. The former is the probability that the pair can be successfully established between the end-users while the latter is the probability that the pair is actually suitable for teleportation. The tuple (η, p) is defined as the *cost-vector* of the pair. The main utility of this formalism is that quantum routing protocols can be re-cast as *edge reductions on a multi-graph*. Specifically, we will show that swapping operations correspond to path contractions while purification operations collapse multiple edges on the same vertices to a single edge. We begin this section by deriving these contraction rules for a specialised networking scenario and conclude with a holistic analysis about our framework.

A. Entanglement distribution

The first step in our cost-vector formalism is to construct the multi-graph corresponding to the initial state of our network. We recall from our discussion in section I.A.2 that entangled pairs should be distributed no further than the nearest neighbors. We therefore imagine the *initial state* of the network as the point immediately after attempting entanglement distribution between each neighboring pair of vertices. More generally, we imagine this taking place over a small time interval Δt. Depending on the length of Δt, the computers of the network may have attempted to deliver entangled pairs one or more times. Each attempt is then represented in the multigraph as an edge connecting the corresponding vertices with a *cost-vector* that depends on the channel. With this multi-graph, we can now begin routing entanglement by contracting the edges with the swapping and purifying protocols we're about to describe.

B. Entanglement swapping

Suppose we have a network path consisting of n sequential channels. For the sake of example, let us suppose these are all partially depolarizing channels with coherence probabilities $p_1, p_2, \cdots, p_n$ and transmission probabilities $\eta_1, \eta_2, \cdots \eta_n$ respectively. The cost-vectors corresponding to these channels are then $(\eta_1, p_1), (\eta_2, p_2), \cdots, (\eta_n, p_n)$. When two pairs with transmission probability η_1 and η_2 are *deterministically swapped*, the transmission probability of the output pair is $\eta_1\eta_2$ since both pairs must exist for the swapping to take place. The transmission probability for swapping along the entire path is therefore $\eta_1 \times \eta_2 \times \cdots \times \eta_n$. More generally, we might imagine that each swapping operation has some identical probability of failure η_{swap}, which gives a new overall success probability of

$$\eta_{\text{swap}}^n(\eta_1 \times \eta_2 \times \cdots \times \eta_n) \tag{3.1}$$

We recall from theorem 2, that the coherence probability of a pair distributed along a path is the product of the coherence probabilities of the channels in that path. The cost-vector of the reduced path is therefore

$$\Big(\eta_{\text{swap}}^n(\eta_1 \times \eta_2 \times \cdots \times \eta_n),\ \ p_1 \times p_2 \cdots \times p_n\Big) \tag{3.2}$$

C. Entanglement purification

An entanglement purification protocol takes a number of partially entangled states and uses local operations and classical communications to reduce the initial ensemble to a smaller number of states that more closely resemble some maximally entangled reference state. Considerable work has been done to find protocols that maximize the attainable yield of target states for finitely many initial states or bound the yields that are attainable in asymptotic settings. A notable result in this area is that there is a one-to-one correspondence between purification protocols on entangled pairs and CSS codes (Bennett *et al.*, 1996b). Here, we limit our attention to the *Bennett protocol* (Bennett *et al.*, 1996a) which is the simplest instance of a CSS-type purification; It is capable of *detecting* the presence of a single Pauli error (for example the bit-flipped pair $(I \otimes X)|\phi^+\rangle = |\psi^+\rangle$). The Bennett protocol essentially works by coupling two pairs together and destructively measuring one of them to learn whether there was a Pauli error on either of the pairs. If a Pauli error was detected, the remaining pair must be discarded since there is complete uncertainty about where the error could have occurred. On the other hand if no error was detected, the remaining pair is kept. In this section, we show how the Bennett protocol acting on *partially dephased states* can be easily adapted to the cost-vector formalism. In short, this is because partially dephased states only suffer one kind of Pauli error which makes them naturally suited for this type of purification. Following this, we briefly consider Bennett purification on partially *depolarized states* and demonstrate how it can be adapted to the cost-vector formalism with an additional post-processing assumption.

1. Partially dephased pairs

Let us begin by considering two *partially dephased pairs* with pair fidelities F_1 and F_2 The fidelity of the pair that passes the Bennett purification is given by

$$F' = \frac{F_1 F_2}{F_1 F_2 + (1-F_1)(1-F_2)} \tag{3.3}$$

and the success probability of the protocol is given by the denominator:

$$\eta_{\text{pur}} = (F_1 F_2 + (1-F_1)(1-F_2)) \tag{3.4}$$

We recall from section II.D that that the fidelities for partially dephased and partially depolarized states can both be related to coherence probabilities. Substituting F_1 with $(1+p_1)/2$ and F_2 with $(1+p_2)/2$ respectively (according to theorem 4) gives us

$$\begin{aligned} \frac{1+p'}{2} &= \frac{(1+p_1)(1+p_2)}{2+2p_1p_2} \\ p' &= \frac{p_1+p_2}{p_1p_2+1} \end{aligned} \tag{3.5}$$

Here, p' is the coherence probability of the new partially dephased state. Relating the success probability in terms of coherence probabilities:

$$\eta_{\text{pur}} = \frac{1}{2}(1+p_1p_2) \tag{3.6}$$

And we are now ready to present how cost-vectors are updated when two parallel edges are contracted by a Bennett purification. Let (η_1, p_1) and (η_2, p_2) be the cost-vectors of two partially dephased pairs that are shared a pair of end-users. Evidently, the coherence probability of the resulting purification is given by eq. 3.5. The overall success probability is the probability of the purification protocol taken with the product of each transmission probability (since both pairs must exist for the purification to be attempted). The resulting cost-vector is therefore

$$\left(\frac{1}{2}\eta_1\eta_2(1+p_1p_2),\ \ \frac{p_1+p_2}{p_1p_2+1}\right) \tag{3.7}$$

2. Partially depolarized pairs

Similar to previous section, we begin by considering two partially depolarized pairs with pair fidelities F_1 and F_2. The fidelity of the output pair in this case is

$$F' = \frac{F_1F_2 + \frac{5}{9}(1-F_1)(1-F_2)}{F_1F_2 + \frac{1}{3}F_1(1-F_2) + \frac{1}{3}F_2(1-F_1) + \frac{5}{9}(1-F_1)(1-F_2)} \tag{3.8}$$

Unlike in the previous example where the output pair was a partially dephased state like its inputs, the output pair here does not have the form of eq 2.2. Rather, it has a skewed distribution of errors. This is because the Bennett protocol only detects one type of Pauli error at a given time (X or Z). For the cost-vector formalism to work, we must convert this state back to a partially depolarised pair. This can be done with *entanglement twirling* which equalises the noise terms using random local operations. The drawback of this approach however is that states with biased noise are much easier to purify than states with no bias at all. This means we have to expend some of our distillable entanglement in order to be consistent with our cost formalism in this scenario.

Substituting F_1 with $(1+3p_1)/4$ and F_2 with $(1+3p_2)/4$ respectively (according to theorem 3) gives us,

$$\frac{1+3p'}{4} = \frac{3-p_2+p_1(7p_2-1)}{4+4p_1p_2}$$
$$p' = \frac{2-p_2+p_1(6p_2-1)}{3+3p_1p_2} \tag{3.9}$$

Where, as before, p' is the coherence probability of the new state. Substituting again, the success probability of the purification is

$$\frac{1}{2}(1+p_1p_2) \tag{3.10}$$

And the resulting cost-vector is

$$\left(\frac{1}{2}\eta_1\eta_2(1+p_1p_2),\ \ \frac{2-p_2+p_1(6p_2-1)}{3+3p_1p_2}\right) \tag{3.11}$$

D. Entanglement stacking

In the previous section, we demonstrated how entanglement purification can be used in our cost-vector formalism to combine concurrent edges into a single edge with a higher coherence probability. Here, we introduce a complimentary strategy called *entanglement stacking* which combines concurrent edges into a single link with a higher transmission probability. First, let us recall that the edges of our multi-graph represent entangled pairs *that could exist* in the network. We can choose to represent a collection of edges that are shared by a pair of users as a single link with a higher overall success probability. This simplifies the graph topology, but comes at the expense of some accuracy since removing edges means disregarding the possible existence of other legitimate pairs. Unlike with swapping and purification, we emphasise that there is no physical process that takes place during entanglement stacking.

Here, we propose a rudimentary entanglement stacking protocol on two edges with cost-vectors $v_1 = (\eta_1, p_1)$, and $v_2 = (\eta_2, p_2)$ respectively. For the sake of example, we suppose these are cost-vectors specifying partially depolarized states. Let η' denote the transmission probability of the stacked edge, and let it be defined as the probability that at least one of the two pairs are successfully transmitted. Then,

$$\eta' = \eta_1\eta_2 + \eta_1(1-\eta_2) + \eta_2(1-\eta_1) \tag{3.12}$$

If one pair is transmitted, the end-users receive the v_1 state with probability $\gamma_1 = \frac{\eta_1}{\eta_1+\eta_2}$ and the v_2 state with probability $\gamma_2 = \frac{\eta_2}{\eta_1+\eta_2}$ The resulting mixed state is therefore:

$$\gamma_1(p_1|\phi^+\rangle\langle\phi^+| + \frac{1}{4}I(1-p_1)) + \gamma_2(p_2|\phi^+\rangle\langle\phi^+| + \frac{1}{4}I(1-p_2)) \tag{3.13}$$

Expanding and rearranging gives us,

$$(\gamma_1p_1+\gamma_2p_2)|\phi^+\rangle\langle\phi^+| + (\gamma_1(1-p_1)+\gamma_2(1-p_2))\frac{1}{4}I \tag{3.14}$$

Which is another partially depolarized state with coherence probability

$$p' = \gamma_1p_1 + \gamma_2p_2 \tag{3.15}$$

The cost-vector of the stacked path is therefore

$$\left(\eta_1\eta_2 + \eta_1(1-\eta_2) + \eta_2(1-\eta_1),\ \ \gamma_1p_1 + \gamma_2p_2\right) \tag{3.16}$$

Although we do not treat on this subject any further, we remark that there appears to be good potential for developing more general stacking protocols. Rather than stacking up to a single pair for example, it may be preferable to develop a scheme for stacking n pairs into $m < n$ pairs as a more nuanced simplification.

IV. ENTANGLEMENT ROUTING OVER TIME

Although the cost-vector formalism in its current iteration might be sufficient for routing between a small number of end-users, we will later see that congestion quickly becomes an issue as the number of users increases. Network congestion occurs because of *path collisions* where two or more parties are separated by a common *bottleneck*. Since it is impossible for all parties to send messages through a bottleneck simultaneously, some parties must wait until the channel frees up or another path becomes available. In the context of quantum networking, path-collisions occur when two or more parties need to swap over the same entanglement link. Similarly, these kinds of collisions are resolved by having parties wait until new links are established. This waiting action can (and should) be treated as a quantum channel since holding qubits in memory always introduces a small amount of unintended noise. In this section, we demonstrate how our cost-vector formalism can be extended to networking scenarios where states may be stored in *quantum memories*. In brief, our main insight is that multi-graphs representing distributed entanglement are extended in time by adding duplicate layers that describe the network in increments of Δt. Edges between layers represent *memory channels* that carry quantum states across time. Temporal routing protocols are then recast as edge-reductions on this larger multi-graph.

A. Memory channels

We recall from section I.A that a quantum network is defined as a collection of quantum computers that are interconnected according to a graph of single qubit error channels. These *transport channels* allow qubits to be moved across the computers of the network. Quantum memories on the other hand can be thought of as channels that *move qubits through time*. A precise, mathematical description of this is beyond the scope and utility of this paper, so we simplify by supposing that every qubit can be assigned a label indicating its position in time. For example $\rho_{t=x}$ would correspond to the state ρ at a time x where time is measured in units of Δt (See sec. III.A). The action of an *ideal memory channel* $\mathcal{E}_{\text{mem}}$ is then defined

$$\mathcal{E}_{\text{mem}}(\rho_{t=x}) = \rho_{t=x+1} \tag{4.1}$$

In practice, memory channels are imperfect since they represent real-world processes. As with transmission channels, we consider a simplified picture of quantum memories by supposing they are either *partially depolarising channels* or *partially dephasing channels* with a coherence probability p and a transmission probability η.

B. Transitory pairs

The fact that we can specify a p and η for our memory channels strongly suggests there is some way of incorporating memories into the cost-vector formalism. It is not immediately obvious though how this ought to be done. We recall from section III that the edges of our multi-graph represent entangled pairs that could exist in the network by following some sequence of purification and swapping operations. At face value, this seems to rule out the possibility that memory channels could be represented with edges. In this section however, we propose a fictitious category of states called *transitory pairs* that allow us to treat memory channels as states that are partially entangled *over time*. From this, we show how memory usage can be recast as entanglement swapping.

To begin, let us suppose we have an ideal memory channel $\mathcal{E}_{\text{mem}}$ as defined in equation 4.1. We now imagine the hypothetical scenario where this channel is applied to one half of a $|\phi^+\rangle$ pair at some initial time $t = 0$. This corresponds to a *non-physical* process where one of the particles is moved forward in time while the other stays behind. The resulting *"state"* is therefore

$$|\phi^+_{\Delta t}\rangle := \frac{1}{\sqrt{2}}\Big(|0\rangle_{t=0}|0\rangle_{t=1} + |1\rangle_{t=0}|1\rangle_{t=1}\Big) \tag{4.2}$$

More generally, if the memory channel is partially depolarizing (dephasing), the state will be a partially depolarized (dephased) pair where the qubits are seperated by one time unit. For example, a partially depolarizing channel applied to one half of $|\phi^+\rangle$ would result in the object,

$$\rho_{\Delta t} = p[\phi^+]_{(t_1=0,\, t_2=1)} + (1-p)\frac{1}{4}I_{(t_1=0,\, t_2=1)} \tag{4.3}$$

Where t_1 and t_2 are the positions in time of the first and second particle respectively. Objects of this type, where the qubits of the underlying state are positioned at different times, we call *transitory pairs*. This name was chosen to emphasise the fact that these pairs are partway through a larger time-evolution and, as such, do not currently represent resources that can be used for teleportation. To illustrate this point more clearly, consider the time-evolution

$$\mathcal{E}_{\text{mem}} \otimes \mathcal{E}_{\text{mem}}\Big(|\phi^+\rangle_{(t_1=0,t_2=0)}\Big) = |\phi^+\rangle_{(t_1=1,t_2=1)} \tag{4.4}$$

Clearly, this is a valid physical process since it pushes the entire $|\phi^+\rangle$ state one step forward in time. Nevertheless, we can decompose this process to obtain a *transitory pair* midway through the calculation.

$$(\mathcal{E}_{\text{mem}} \otimes \mathcal{I})(\mathcal{I} \otimes \mathcal{E}_{\text{mem}})\Big(|\phi^+\rangle_{(t_1=0,t_2=0)}\Big) \tag{4.5}$$

$$= (\mathcal{E}_{\text{mem}} \otimes \mathcal{I})|\phi^+_{\Delta t}\rangle \tag{4.6}$$

For a transitory pair to be converted into a teleportation resource, it must find one or more memory channels that can bring both of its qubits to the same position in time. If this is not possible (because there are no available memories), the state is considered lost.

C. Temporal swapping

In the previous section, we defined the transitory pairs and suggested that using memory channels is equivalent to a swapping operation on transitory pairs that have been *"distributed"* through memory channels. Let us begin by first defining the swapping operation over transitory pairs. Our intuition informs us that a swapping operation should only be possible if the two qubits being measured exist at the same time. Therefore let $\rho_{t_1=a,t_2=b}$ and $\sigma_{t_1=b,t_2=c}$ be partially entangled transitory pairs where the second qubit of ρ and the first qubit of σ are both found at time b. The *temporal swapping operation* on these two states is defined by the action

$$\mathcal{T}(\rho_{(t_1=a,\, t_2=b)} \otimes \sigma_{(t_1=b,\, t_2=c)}) = \mathcal{E}_{\text{swap}}(\rho \otimes \sigma)_{(t_1=a,\, t_2=c)} \tag{4.7}$$

For the remainder of this section, we demonstrate the equivalence between memory usage and temporal swapping over transitory pairs. Imagine that two parties Alice

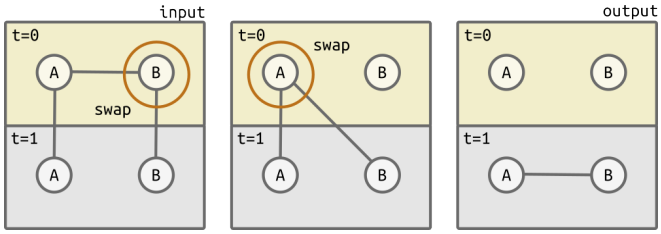

Figure 2: A simple routing protocol consisting of two temporal swaps. The initial state of the network is presented in the left-most square. At time $t = 0$, Alice and Bob share an entanglement link between them and each posses a transitory link which indicates availible quantum memory. The protocol begins by swapping the links at Bob's vertex at $t = 0$. The resulting entanglement is a transitory pair that extends from Alice to Bob one time-step into the future. Swapping the entanglement at Alice's position results in a genuine resource between Alice and Bob at $t = 1$.

and Bob share a $|\phi^+\rangle$ state and want to keep this pair in memory for one unit of time using partially depolarizing memory channels with coherence probabilities p_A and p_B respectively. The resulting state is easily verified to be

$$\mathcal{E}_d(p_1) \otimes \mathcal{E}_d(p_2)(|\phi^+\rangle\langle\phi^+|) = \Delta_{p_1 p_2} \tag{4.8}$$

Now let us treat the scenario from the perspective where, instead of applying the channel directly, we use the vertex contraction rule developed for swapping in the in the cost-vector formalism to determine the final state. Our swapping strategy is presented diagrammatically in figure 2. Initially, a single link exists between Alice and Bob at $t = 0$ with the cost-vector $(\eta = 1, p = 1)$. The first swapping operation (marked by the circle on $B_{t=0}$) results in a partially depolarized transitory pair between Alice at $t = 0$ and Bob at $t = 1$. Using the update rule derived in equation 3.2, the transitory pair has the cost-vector $(1, p_A)$. Swapping again on Bob's vertex and applying the same update rule results in a partially depolarized pair at $t = 1$ with a cost vector of $(1, p_A p_B)$, which is the same state described in equation 4.8. From this, we conclude that temporal swapping operations are equivalent to uses of memory channels.

One counter-intuitive feature of our time-dependent formalism is that network paths do not have to descend monotonically but can weave forwards and backwards in time. Although this might appear nonsensical at first, *some* of these paths nevertheless represent physically realisable quantum routing protocols. To illustrate, consider figure 3, where a network path between nodes $A_{t=1}$ and $D_{t=1}$ appears to jump up briefly to $t = 0$. What the path indicates in reality is that $B_{t=0}$ and $C_{t=0}$ have an entangled pair that can be stored in memory for one unit of time. During this time, $(A_{t=1}, B_{t=1})$ and $(C_{t=1}, D_{t=1})$ are able to establish entanglement links. If $(B_{t=0}, C_{t=0})$ had decided to store their pair in memory, a continuous

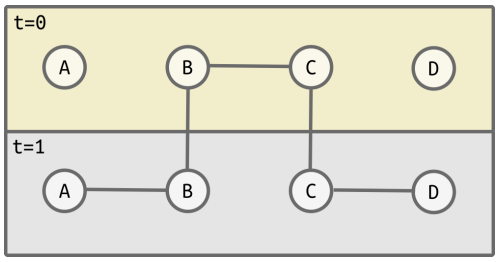

Figure 3: The path of this temporal network, which starts at $A_{t=1}$ and ends at $D_{t=1}$ appears to propagate backwards in time if followed from left to right.

path of entanglement links would exist between A and D at the $t = 1$ time-layer which could be swapped to give them end-to-end entanglement.

There are however instances of temporal paths that *do not* represent realisable routing protocols, some examples of which are presented in the top part of fig. 4. Essentially, there are two conditions that must be met for a path through a temporal network to be valid. The first condition is that the ends of the path must exist at the same time layer. The second condition is that the path cannot push into the future *beyond* the end points of the path. An example of this condition being violated is given in Fig. 4 (II), where a path between $A_{t=0}$ and $D_{t=0}$ utilises a resource at $t = 1$. Such a path breaks causality by implying that a resource available in the future could be used to establish an entanglement link in the present.

D. Temporal purification

Entanglement purification, like entanglement swapping, can be defined over transitory pairs but only in the special case of *one-way purification*. This is a subset of protocols where classical communication is only permitted in a single direction between the two parties. A purification on temporal links carries the interpretation that one party performs their half of the protocol with the intent to signal their measurement outcomes to a recipient at some later time.

E. Constructing the temporal meta-graph

We recall from section III.A that the state of a network after some time Δt can be represented as a multi-graph G where each edge is a potential entanglement link weighted with a corresponding cost-vector. Our objective now is to construct multi-graphs that encode *entanglement and memory resources* over n intervals of Δt. We call these structures *temporal meta-graphs* to distinguish them from the multi-graphs that only represent entanglement resources. To build a temporal multi-graph, we begin by initialising n copies of G where each graph represents the

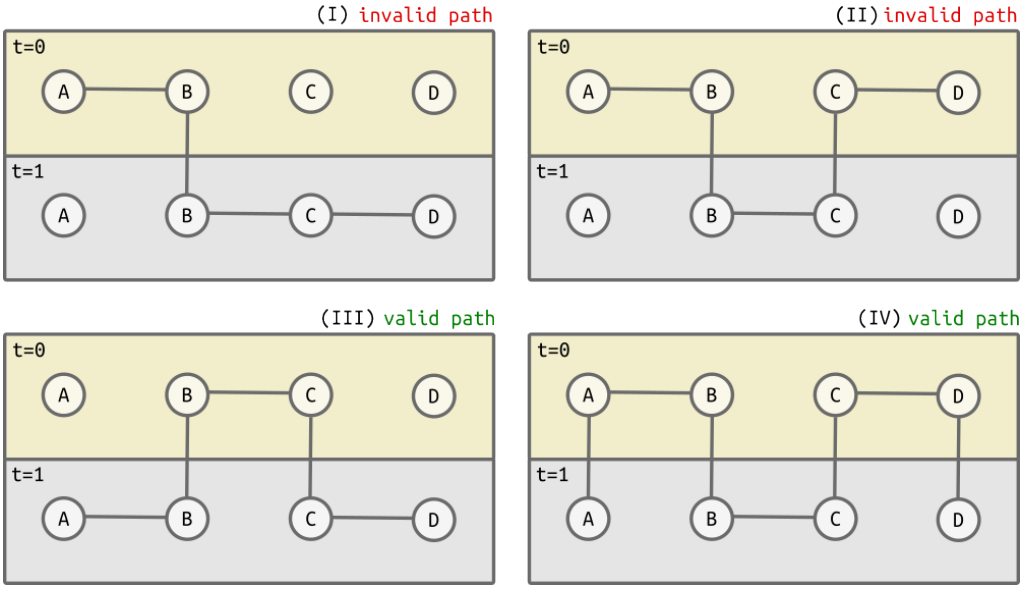

Figure 4: Four examples of valid and invalid temporal paths connecting two vertices A and D. Two conditions must be met for a path to be valid: The start and end points of the path must exist at the same time, and the path cannot ever descend *below* the ends of the path. Sub-figure (I) is an invalid path because the end points are not at the same time layer. Sub-figure (II) is an invalid path because a link between $B_{t=1}$ and $C_{t=1}$ cannot be used to generate a link between $A_{t=0}$ and $D_{t=0}$ (In other words, future resources cannot be used to route entanglement in the past). Sub-figure (III) is a valid path and is reproduced from fig 3. Sub-figure (IV) is a valid path made to resemble path (II). The difference now is that memory links connect A and D which allows them to store their pairs at $t = 0$ and swap at $t = 1$.

entanglement generated in increments of Δt. Following this, we connect each node to itself at the next time layer with a number of transitory pairs equal to the number of available memories. An example construction is illustrated in fig 5.

F. Pathfinding in temporal-metagraphs with asynchronous nodes

Routing protocols for quantum networks will almost certainly rely on path-finding subroutines to find optimal paths between two vertices according to some heuristic. This is an issue for temporal meta-graphs since multiple vertices can represent the same user at different times. We present one possible solution to this problem by introducing so-called *asynchronous nodes*. These are vertices that are temporarily added to the meta-graph for the duration of a path-finding protocol and are exclusively connected to the vertices representing a single user (See Fig. 6 and Fig. 7 for examples). By adding asynchronous nodes that correspond to a pair of users, path-finding algorithms are able to discover the optimal path between them over the entire temporal meta-graph.

One issue with this approach however is that a found path *is not necessarily valid* according to the two conditions given in section IV.C. Specifically, the end-points of a found path may exist at different times or the path may dip below the end-points (See 7). Both of these problems are rectified if Alice and Bob are both allocated additional memory channels *in advance* to ensure the ends of their path terminate at the same time and at the appropriate depth. A relatively easy (though simplistic) implementation of this solution is to assume that Alice and Bob each have a *reserve supply* of quantum memories that are not included in the description of the temporal meta-graph. This way, if an invalid path between asynchronous nodes is discovered, the reserve memory can be automatically allocated to ensure the path is physically realisable.

The edges connecting asynchronous nodes to their counterpart vertices may also be weighted with cost-vectors in order to prioritise access to certain time-layers. For example, it may be that the asynchronous edges pointing to lower time-depths are highly penalised to create an incentive for faster routing. Alternatively, if a layer is known to be congested, it may be preferable to prioritise paths that start at a different layer. The flexibility of this approach may prove advantageous in the development of quantum routing algorithms that incorporate load balancing.

V. MULTI-PATH ROUTING

A quantum network, like any other communications network, may be circuit-switched or packet-switched. A *circuit-switched* network is one where the end-users reserve network paths for the duration of their communication. This model is well-suited for routing entanglement in

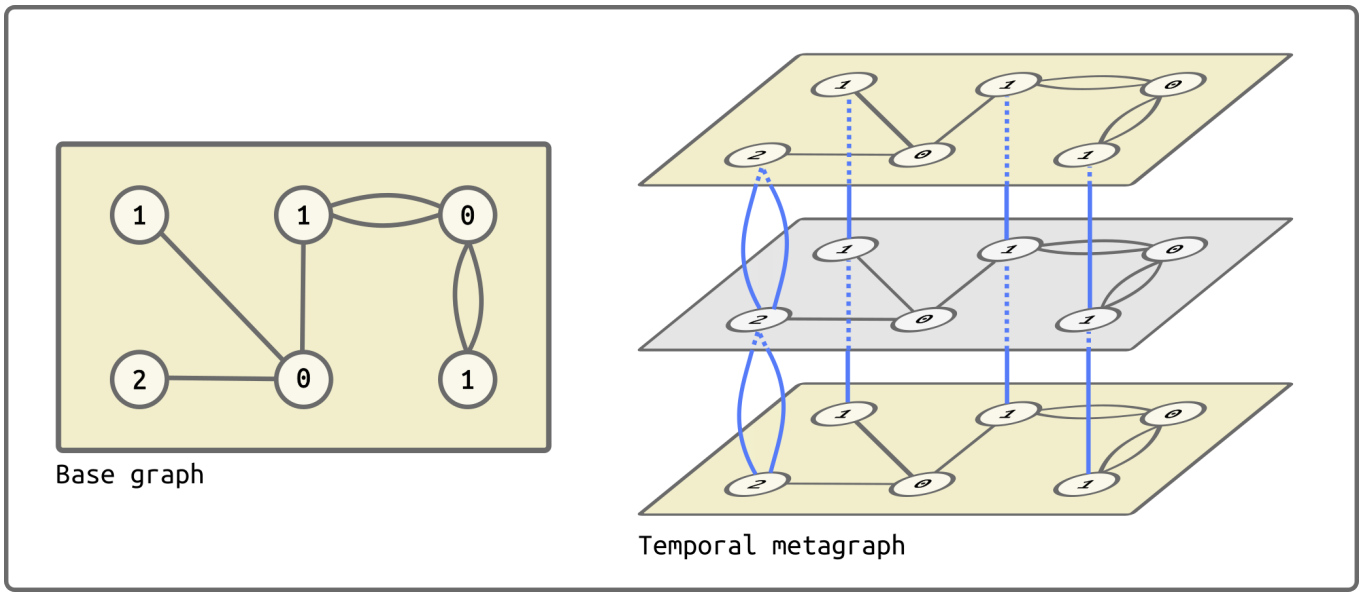

Figure 5: Left: An arbitrary multi-graph where edges are potential entanglement links. The numbers of the vertices indicate how many quantum memories exist at that location. Right: A temporal multi-graph corresponding to the base graph over three time-layers. Three instances of the original graph are connected by transitory pairs corresponding to the number of memories at each vertex.

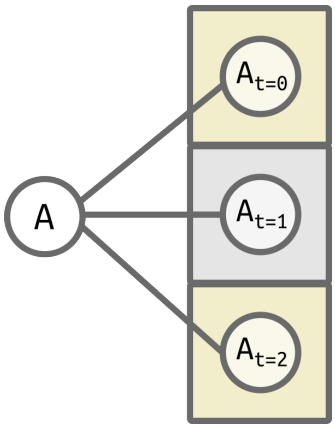

Figure 6: An example of an *asynchronous node* (left) for some network party Alice. This node has edges between all vertices that represent Alice at different times.

the *link-level* paradigm, since high fidelity pairs must be established along a fixed path. Compare this to the *packet-switching* picture where data is routed over many different channels subject to availability. This approach is favored by the *end-level paradigm* where there is flexibility in the paths that can be taken. Moreover the packet-switching paradigm allows for the possibility of routing over *multiple paths simultaneously*. In this section, we introduce rudimentary greedy algorithms for multi-path routing in the end-level paradigm of our cost-vector formalism involving one or more pairs of end-users. We emphasise that these algorithms are unlikely to be optimal in most scenarios, particularly in cases where multiple users must route together. Nevertheless, we will see in the latter part of this paper how even these basic protocols can allow us to make a number of important insights into the design principles of quantum networks.

A. One user-pair

Our greedy algorithm for multi-path routing on one user-pair is outlined in the textblock labeled Alg. 1. We begin with a cost-vector multi-graph G, a pair of end-users and a small positive number ϵ which indicates the pair infidelity we hope to attain. Essentially, the strategy of this algorithm is to find the best path on the graph G with respect to the coherence probability p. Once this path is found, it is reduced to a single link by swapping the intermediate vertices. If the fidelity of this link is within the threshold, (i.e. if $F(\text{link}, |\phi^+\rangle \geq 1-\epsilon)$ the protocol ends. Otherwise, the next best path is reduced and the two links are purified to one using the Bennett protocol discussed in section III.C. This repeats until either the resulting link exceeds the fidelity threshold or there are no more paths between the users.

B. Multiple user-pairs

Our algorithm for multi-path routing with multiple users is similar to our previous algorithm, and is presented in Alg. 2. The only significant difference is that we attempt to balance requests by allocating paths to each user sequentially. In other words, we find a path for the

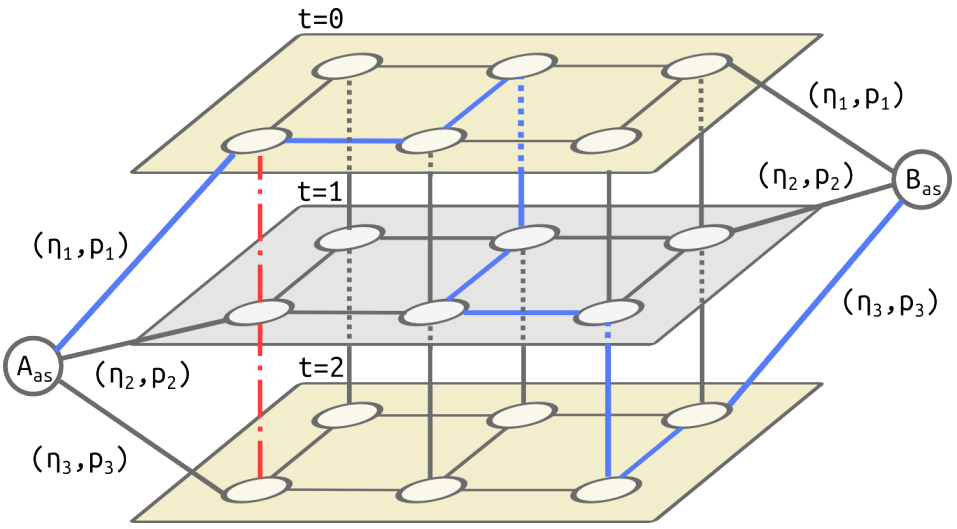

Figure 7: A temporal meta-graph with two asynchronous nodes A_{as} and B_{as} representing parties A and B. The edges connecting the asynchronous vertices may be weighted with arbitrary cost-vectors depending on how one wants to prioritise access to different time layers. An example (though not necessarily optimal) path between the asynchronous nodes is highlighted in blue. Although this path connects A_{as} and B_{as}, it does not currently correspond to a physically realisable communication protocol since the "start" of the path (the first vertex after A_{as}) is at time $t = 0$ while the "end" is at $t = 2$. Nevertheless, the path can be treated as valid provided that Alice is promised a secure memory channel from $t = 0$ to $t = 2$ (this is marked with a red dash-dotted line).

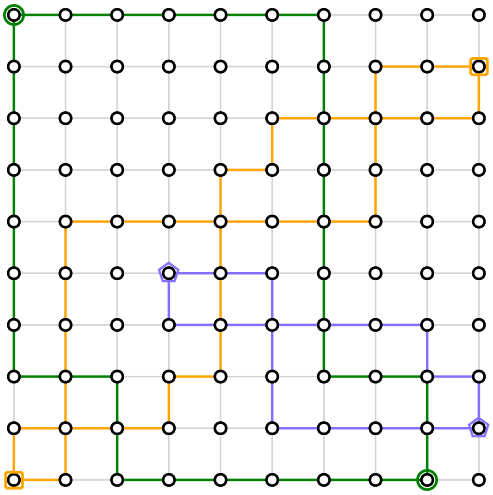

Figure 8: The outcome of Alg 1 when applied to an instance of a 10×10 grid with three randomly selected pairs of end-users (marked with circles, squares and pentagons respectively). All edges are equally weighted.

input : cost-vector multi-graph G, user_pair, threshold ϵ.
output : (if successful) a partially entangled link between the users of user_pair with pair fidelity above $1 - \epsilon$

begin
  while *paths exist between user_pair* **do**
    p = `best_path_wrt_coherence(`G, *user_pair*`)`
    link = `swap_path(`p`)`
    if *user_pair already has link* **then**
      link = `purify(`*link, old_link*`)`
    if $F(\text{link}, |\phi^+\rangle) \geq 1 - \epsilon$ **then**
      return link *(success)*
  return link *(fail)*

Algorithm 1: A greedy algorithm for multi-path entanglement routing between a single pair of end-users. For context, note that p is the optimal path connecting the end users with respect to *coherence probability*.

first users, then find a path for the second users, and so on, before looping through the users again. This continues until either each user is able to purify a link to the fidelity threshold or there are no more paths remaining between any of the users.

VI. BENCHMARKING

Characterising the performance of a routing algorithm, whether quantum or not, is an exceptionally difficult research challenge. The first and perhaps most significant obstacle is that it is not obvious how performance ought to be scored, since there are many (if not innumerably many) valid options for doing so. The second problem is that the performance of a routing algorithm will inevitably depend on the topology of the network and the underlying *demand*

```
input  : cost-vector multi-graph G, end_users,
         threshold ϵ.
output : (if successful) partially entangled links
         between every end-user each with pair fidelity
         above 1 − ϵ
begin
    while end_users have paths do
        for end_users with paths do
            p = best_path_wrt_coherence(G,
              end_user)
            link = swap_path(p)
            if end_user already has link then
                link = purify(link, old_link)
            if F(link, |ϕ+⟩) ≥ 1 − ϵ then
                remove end_user from list # they've got
                  a good pair!
    if all users have good pairs then
        return links (success)
    else
        return links (fail)
```

Algorithm 2: A greedy algorithm for multi-path entanglement routing between multiple end-users.

function which models how and when users make requests to the network. This is less of a concern in the classical context since simulated networks can be modeled after networks in the real world. We, on the other hand, have no such luxury since quantum networks do not currently exist at scale. For simplicity therefore, we limit ourselves to a toy model of quantum networking where the vertices of the network are arranged in a grid with equally weighted edges (See Fig. 8) and where the demands of the network are specified by a random selection of n user-pairs who request entanglement links without imposing any demands on the required quality. We quantify the performance of our greedy algorithms by considering the average fidelity of the delivered pairs in tandem with the average efficiency at which they are delivered.

We begin in section VI.A by investigating the average case performance of our multi-path algorithm for a single pair of users. Although this may seem to be a mundane exercise, we observe a surprising amount of combinatorial complexity which demonstrates the effectiveness of random sampling over naive analysis for quantifying network performance. Following this in section VI.B, we study the effectiveness of our routing algorithm when multiple users are competing simultaneously. In doing this, we identify a *saturation point* in which adding more users results in diminishing returns on performance. Finally, in sections VI.C and VI.D we investigate how network congestion is ameliorated by either scaling the network in size or extending the network in time respectively. Our findings indicate the latter approach is considerably more effective.

The scripts used to execute these simulations together with the source code can be found at https://github.com/FalafelGood/QuNet

A. Benchmarking multi-path purification with single-user networks

We begin by studying the average case performance of Alg. 1 for a single pair of users in a square lattice graph (See Fig. 8) of variable size where each edge represents a *partially dephased* pair with a cost-vector of $(\eta = 0.794,\ p = 0.897)$. These seemingly arbitrary values are an artifact of an earlier version of this paper where we described our costs in units related to decibels. In each trial, we randomly select a user pair from the network and use Alg. 1 to establish an entanglement link using a number of paths up to some specified maximum. We present our results for this scenario in Fig. 9. The average fidelity and transmission probability of the distributed pair are given in Fig. 9(a). Because the Bennett purification protocol is non-deterministic, we see the fidelity increase with successive purifications at the cost of decreasing transmission probability. We also observe that both the fidelity and efficiency decrease with grid size since the average distance between random users increases. For a square lattice, the average number of steps between two vertices (also known as the Manhattan distance) is $\frac{2}{3}n$ (See App. B for a derivation). By plotting the fidelity and transmission probabilities on a log scale (Figs. 9(b,c)) we confirm that, as the size of the grid increase, the fidelity and efficiency decay exponentially towards their asymptotic values of $\frac{1}{2}$ and 0 respectively. We observe minor deviations from this trend (particularly in Fig. 9(c)) for small grid sizes which we attribute to *boundary effects*. Specifically, the users in small grids are more likely to be located on the edges or corners of the lattice which limits the number of paths they can use for routing.

We now focus on analytically validating our data, which proves to be a challenging task even in this relatively simple scenario. For a single path, Fig. 9 shows that our numerical data agrees exactly with a simple analytical prediction where the overall cost of the path is calculated as a function of the average Manhattan distance. Allowing for multiple paths however introduces three effects that complicate the analysis. Firstly, the lengths of available network paths depend on whether the end users lie in the same row or column. To illustrate, let L be the Manhattan distance between two users where neither party is located on a boundary of the lattice. The four shortest edge-disjoint paths connecting them will have lengths $(L, L+2, L+2, L+8)$ for users in the same row or column, and $(L, L, L+4, L+4)$ otherwise. The chances of selecting a user pair in the same row or column diminishes quadratically with grid size, and this fraction can be neglected if the grid is sufficiently large. The second complicating effect is that users on the network boundaries have fewer

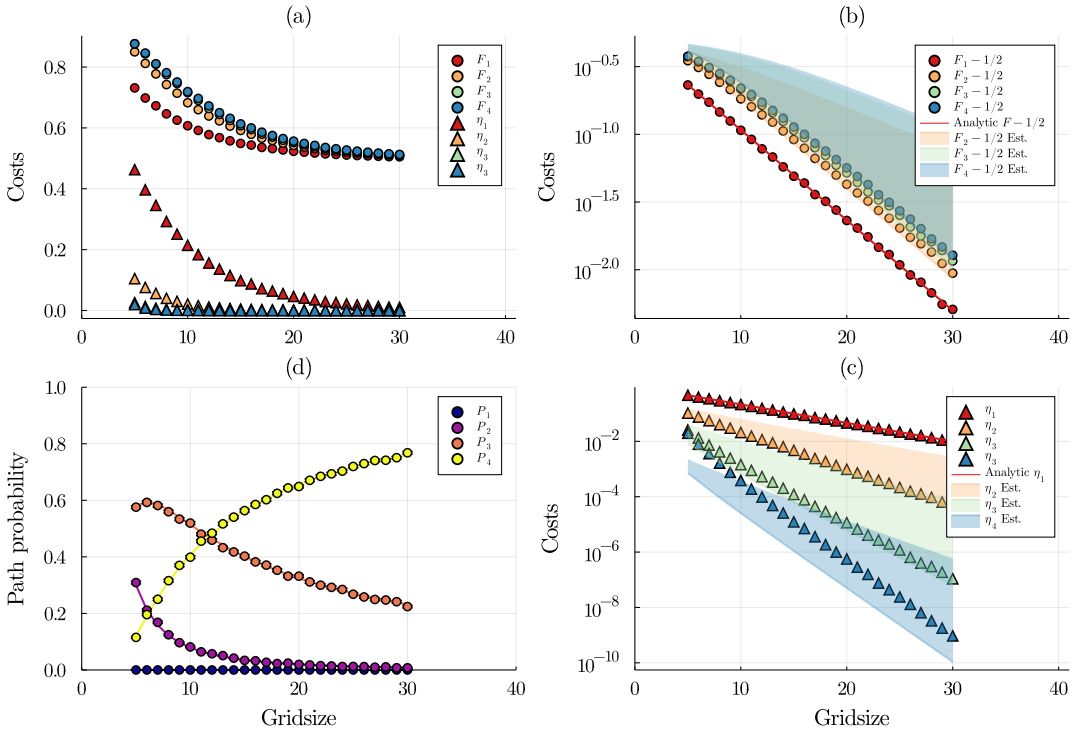

Figure 9: Single-user network performance versus grid size for different numbers of maximum allowed (edge-disjoint) paths. For each trial run, one random user pair was selected on a $n \times n$ rectangular lattice and was routed using `greedy_multi_path`. Each edge is weighted with the cost-vector ($\eta = 0.794, p = 0.897$), and each data point is the average of 5000 random trials. **(a)** Average routing costs in terms of efficiencies η_j and fidelities F_j, where j is the maximum number of allowed paths. **(b, c)** Average costs plotted on a log scale for fidelity $(F_j - \frac{1}{2})$ (b) and efficiency (c). A solid line is plotted for the one-path case where an exact analytical solution is known. For the multi-path cases, the shaded areas show estimated expected scalings for each case, based on analytical approximations. **(d)** Probability P_j that a user finds j paths in the case where up to four paths may be purified. Analytical curves for each path probability are overlaid.

edges and therefore may not be able to use the maximum number of paths permitted by the experiment. Similarly, this effect can be seen in Fig. 9(d) to diminish with grid size.

The third and most significant complication is the non-linear update rule of the Bennett purification (Eq. 3.7). Unlike the previous two effects, the average transmission probability and fidelity of a purified pair cannot be straightforwardly related to the average Manhattan distance, especially when taking the previous two effects into account. Because of this, we elected to compare our multi-path data against two estimates that roughly bound the expected values. These estimates, which define the edges of the shaded regions in Figs. 9(b, c), are calculated by purifying a set of paths with lengths given by the edge-disjoint path sets described above—$(L, L+2, L+2, L+8)$ for users in the same row or column, and $(L, L, L+4, L+4)$ otherwise—with L taken to be the average Manhattan distance for a given lattice size.

B. Multi-user, multi-path routing

Competition between end-users is significant in quantum networks where entanglement resources are scarce. Here, we benchmark the performance of our multi-party algorithm (Alg. 2) for a 10×10 grid lattice with a variable number of random end-users up to the fully saturated limit of 50 user pairs. As in the previous section, each link represents a partially dephased pair with a cost vector of $(\eta = 0.794, p = 0.897)$ though this time we do not impose any artificial constraints on the number of paths that communicants can use. The results of our experiment are shown in Fig. 10.

Fig. 10 (top) shows how the average transmission probability and pair fidelity change with the number of competing user pairs. Starting from the maximal fidelity expected for the 10×10 single-pair case already analysed in Fig. 9, we see the fidelity initially decrease, before flattening out to a steady-state value after approximately 10 user pairs. By contrast, while the efficiency initially increases, it reaches a maximum value at around 10 user pairs, before decaying away towards zero. The initial change reflects the fact that as more users are introduced into the network,

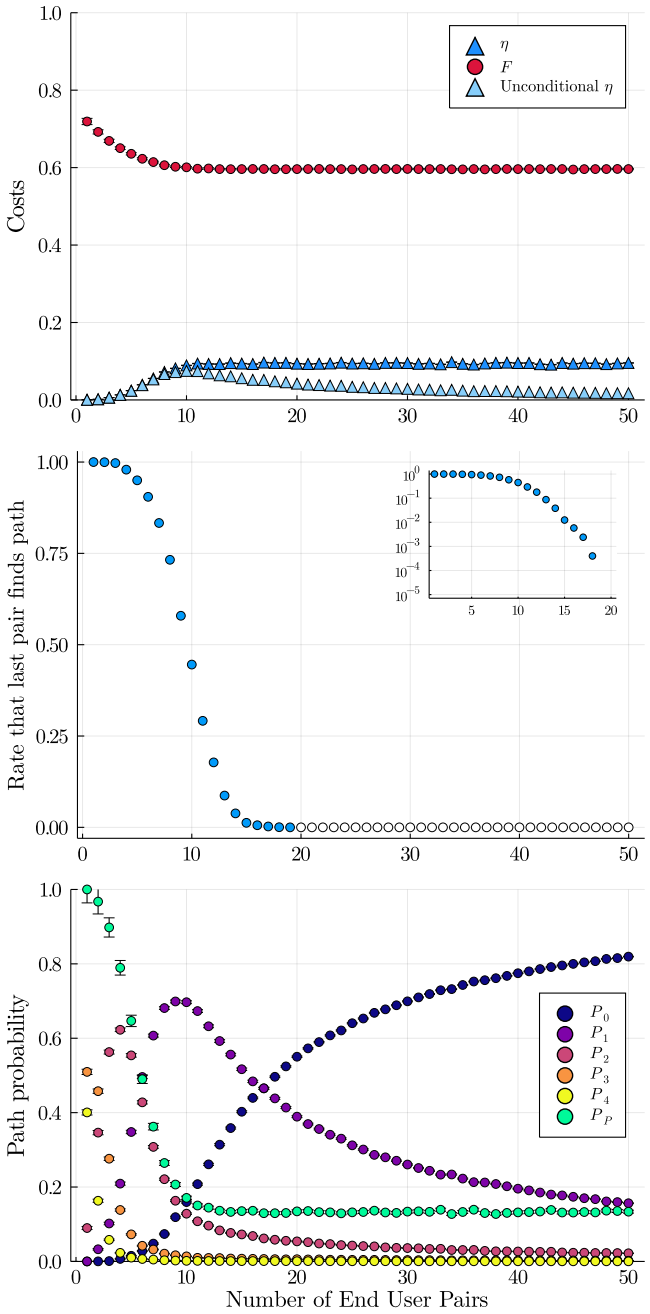

Figure 10: Network performance with the number of competing end users. For each sample, n random userpairs were selected on a 10×10 grid lattice and were routed using `greedy_multi_path`. Each edge is weighted with the cost-vector ($\eta = 0.794, p = 0.897$), and each data point was collected with 5000 samples. (top) Average routing costs in terms of average conditional efficiency η, average conditional fidelity F, and average unconditional efficiency. (middle) The probability that the last userpair queued in `greedy_multi_path` finds at least one path. Unfilled circles are data points where no path was found in the 5000 samples. [top right] log plot. (bottom) Probability P_j that a user finds j paths. P_P is the probability of purification, that is, the likelihood a userpair finds at least two paths between them.

fewer user pairs are able to access multi-path routing, and without the ability to exploit the post-selective purification process, this leads to higher efficiencies, but lower fidelities. In Fig. 10 (bottom), we see that the rates associated with users finding multiple paths all decrease rapidly, and the proportion of users finding only one path increases to a maximum at around 10 user pairs. However, we also see a new effect, arising due to multiuser competition, namely that the proportion of users finding no paths (P_0) increases rapidly after the same point. Thus while the fidelity appears to reach a steady-state value even for large numbers of users, the decaying overall transmission probability for a randomly selected user pair highlights that the network becomes less and less effective at distributing entanglement. To isolate the different factors at play, we also plot a *conditional efficiency cost* in the top figure, where the transmission probability is averaged only over those users who are able to find at least one path. Now, the transmission probability also reaches a steady state value after around 10 user pairs. Our multi-user algorithm (Alg. 2) cycles sequentially through all randomly chosen user pairs (in a fixed order), looking first for one path each, then more paths. Fig. 10 (middle) shows that the rate at which the final user finds at least one path decays very rapidly towards zero, and shows that even though it is possible to choose up to 50 non-colocated user pairs in a 10×10, overall network congestion increases very rapidly and the network capacity effectively reaches full saturation at many fewer user pairs. And once new user pairs can no longer find any new paths, adding users no longer affects how many paths can be found by the other user pairs and the distribution over path numbers remains constant. Indeed, by aggregating the multiple-path rates into a single probability of a user pair being able to access purification, P_P, we see that this probability drops rapidly and monotonically from 1 to a low steady-state value at around 10 user pairs, with the curve closely tracking the shape of the efficiency curve observed in the top panel. These results are consistent with the change in purification rate being the main effect driving the changing path costs in this multiuser setting.

C. Network scaling effects

In the previous sections, we demonstrated how competition can hinder the performance of multi-path entanglement routing. Here, we consider strategies to ameliorate the effects of competition, which we will demonstrate for the case of network congestion. A simple, if perhaps brute-force strategy for mitigating competition is to increase the size of the network. To explore this scenario, shown in Fig. 11, we start with the same fully saturated 10×10 rectangular lattice network with fifty randomly chosen end-users that was studied in Fig. 10, and analyse performance as we increase the size of the network.

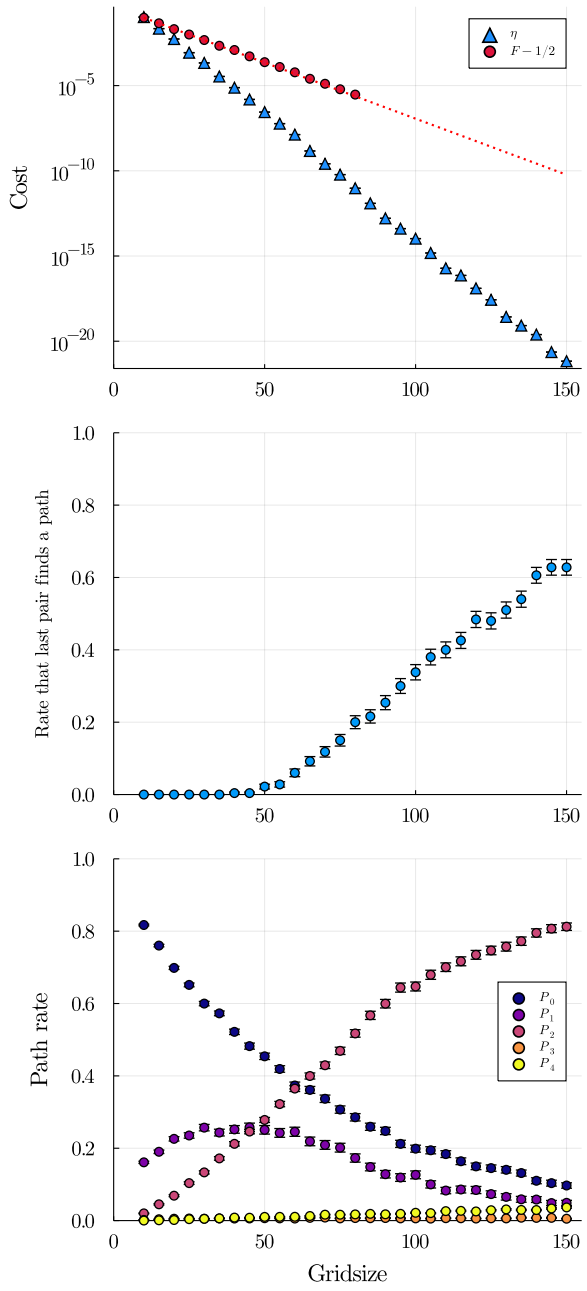

Figure 11: Routing data for fifty randomly chosen userpairs using using `greedy_multi_path` on a grid lattice with variable size. Each edge is weighted with the cost-vector ($\eta = 0.794, p = 0.897$), and each data point was collected with 500 samples. (top) Average multipath routing costs, shown in log scale, for the efficiency η, and fidelity F of the Bell pair (or rather, $F - \frac{1}{2}$). Note that, in log scale, the fidelity data does not show across the full range, because the fidelity rapidly saturates to its asymptotic value of 0.5 beyond the floating point precision used to store the data. (middle) Probability that the last pair is able to find at least one path between them. (bottom) Probabilities of different path finding scenarios such that P_j is the case that j paths were found between the user pair.

As usual, each edge is weighted with a cost vector of ($\eta = 0.794, p = 0.897$). In this scenario, we expect that as we decrease the relative density of user pairs, more links will be routed on average in exchange for a larger average path length. Fig. 11 (top) is a logarithmic plot showing the average routing costs in terms of η and $F - \frac{1}{2}$ versus grid size, the clear linear trends showing the expected exponentially decaying success probabilities with average path length. What is perhaps somewhat surprising is that this effect completely dominates any improvement in congestion that might have been expected to result from increasing the number of paths available for path routing.

As seen in Fig. 11 (bottom), and earlier, for the fully saturated 10×10 lattice, there is more than an 80% chance that a randomly chosen user pair will not be able to find any viable communication pathways. In Fig. 11 (bottom), we also see that the proportion of users that do find paths increases rather rapidly with gridsize. Despite this, Fig. 11 (middle) shows that the rate that the last (50th) user is able to find a path does not start to increase significantly until we reach a grid size around 50×50 (a network 25 times larger than the initial 10×10 case). Even then, this increases rather slowly, not even exceeding 50% until a lattice size around 130×130, by which point the end-user pairs already occupy just a fraction of a percent of the total nodes. The proportion of users finding the most paths (3 or 4) increases even more slowly. Indeed, across the full range, P_3 and P_4 combined only reach around 5%, whereas P_2 (still increasing) reaches in excess of 80%, substantially larger than the maximum P_2 reached in Fig. 10.

By comparison, the probability a random user pair will have the connectivity required to find 3 or 4 paths in principle, is already much larger than 99%. These results indicate that it is much more difficult to unlock paths by expanding the size of a network than it is to increase congestion by adding user pairs. Furthermore, the exponential increase in path costs associated with a larger network, more than counterbalances any potential improvement in multipath routing that the larger network enables. Even when the user-pairs make up a tiny fraction of the total number of nodes, we still find significant competitive effects that limit the multi-path routing capacity. Increasing lattice size is therefore clearly an ineffective strategy for solving network congestion in multipath entanglement networks. In the next section, we explore the alternative paradigm for mitigating congestion with temporal multiplexing, rather than spatial multiplexing.

D. Network Performance with Time-depth

In this section, we use the temporal meta-graph formalism developed in Sec. IV to study how extending a network in time ameliorates congestion. To be consistent with our methodology in the previous section, we again

start with a fully saturated 10×10 lattice graph with 50 user-pairs and analyse the performance of our multi-user algorithm (Alg. 2) as we increase the temporal depth of the meta-graph. In Sec. IV.F we enable path-finding over temporal meta-graphs by temporarily introducing two asynchronous nodes that correspond to a pair of end-users independent of time. Paths found between asynchronous nodes may not necessarily be valid, so we compensate by assuming that each user has a sufficient supply of lossless quantum memories in reserve. Additionally, we assume that every computer in our network has one bit of lossless quantum memory as a publicly available resource. In our previous experiments, a random user pair could use up to a maximum of four paths owing to the fact that the maximum degree of a vertex in a square lattice is four. In order to maintain a fair comparison, we therefore impose a four path limit for each pair in this experiment as well.

We present our results in Fig. 12. The top part of this figure shows the average routing costs of the network versus the maximum depth of the temporal meta-graph. The two dotted lines show the asymptotic "competition-free" values for average efficiency η and fidelity F, respectively, calculated by considering the single-user case with up to five temporal layers available for redundancy. Fig. 12 (bottom) shows the likelihood that a random user-pair will be able to locate zero, one, or more paths between themselves. Here, we find that only a few temporal slices are required to completely eliminate the congestion caused by multi-user competition; Only four time steps are needed for P_0 (the probability of finding no paths) to become negligibly small. Beyond this, we see that network performance continues to improve with increasing temporal depth; Fewer than fifteen layers are necessary to effectively guarantee that every user is able to find the maximum number of allocated paths.

Although our results are conclusively in favour of extending the network in time to improve congestion (as opposed to increasing its scale) it is not clear to what extent the *publicly available* quantum memories contributed to this improvement since users also had the option to begin routing at later times. We study the contribution of quantum memories by considering the average maximum time-depth reached by our multi-user algorithm for two different 10×10 grid networks. The first network has one memory channel available per computer while the other has no public memory channels. If memory channels significantly improve network congestion, then we expect the average maximum time-depth of our routing algorithm to be *smaller* for the network with memories. What we find in Fig. 13, however, is that there is no significant difference between the maximum time-depth reached by the two networks. This suggests that, at least for our greedy algorithm, quantum memories do not significantly improve network performance. Rather, our initial investigation indicates that the effectiveness of temporal routing is primarily because of the freedom to defer path-finding to a less congested layer.

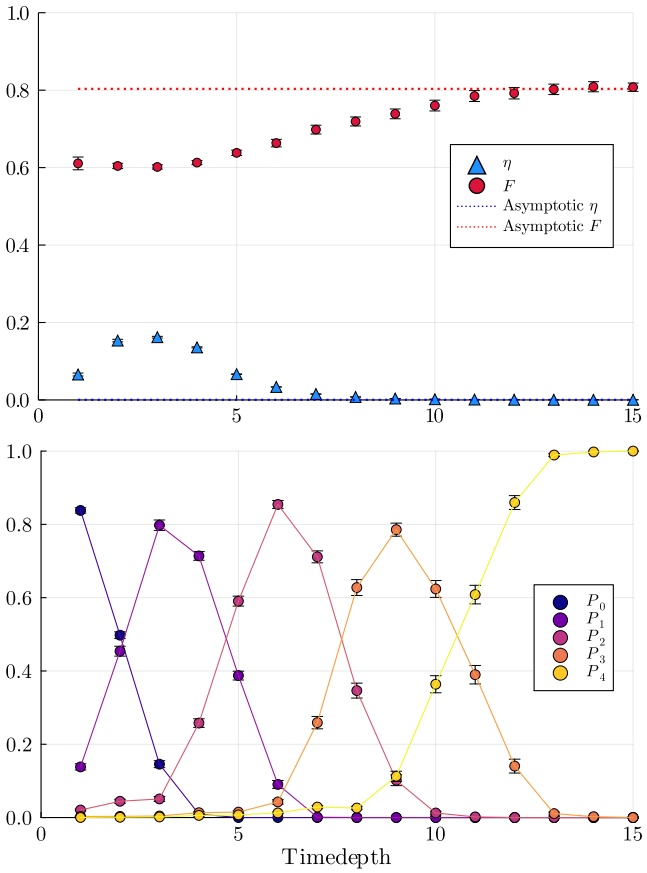

Figure 12: Network performance versus the maximum allowed time-depth. The underlying network is a 10×10 grid lattice that is extended to n distinct temporal layers and 1 asynchronous layer that represents the nodes irrespective of time. Each node is equipped with a lossless quantum memory and so has a directed edge to itself at the next time layer up to the maximum depth. For each sample, a random user pair is chosen at the asynchronous layer and is routed through the temporal network using `greedy_multi_path`. Each edge (Except for those corresponding to lossless memory) Each edge is weighted with the cost-vector $(\eta = 0.794, p = 0.897)$, and each data point was collected with 1000 samples. (top) Average routing costs in terms of the efficiency η, and fidelity F of the Bell pair. The dotted lines are the costs for η and F in the limit where it is assumed each userpair has a time layer to themselves. (bottom) Probabilities of different path finding scenarios such that P_j is the case that j paths were found between the userpair.

VII. CONCLUSION

In this paper, we developed a framework for expressing quantum routing protocols as a series of edge reductions on a multi-graph. We began with a brief introduction of quantum networking and used prior results in the literature to demonstrate the hardness of finding optimal

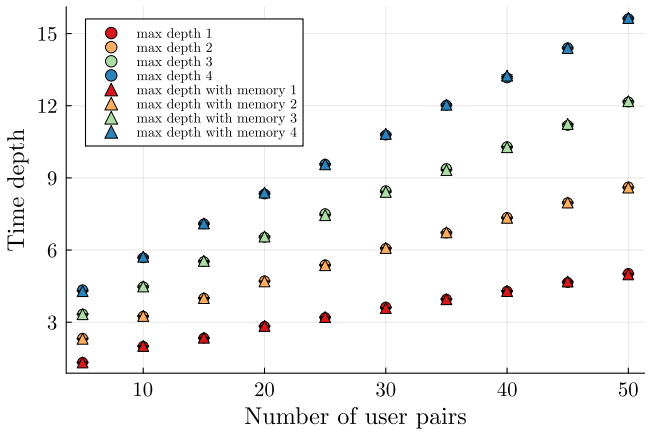

Figure 13: A comparison of the average maximum time depth reached by `greedy_multi_path` for two different networks; Both are 10×10 grids extended in time by 20 layers but one has lossless quantum memories on each node while the other has none. If a node has a memory, there exists a directed edge pointing the node to itself at the next time-layer. The routing between temporal layers is unrestricted, meaning that users may start and finish at any level they like so long as it respects causality. Earlier times are prioritised over later times, and asynchronous routing is prioritised over memory channels. Each edge (Except for those corresponding to lossless memory) Each edge is weighted with the cost-vector ($\eta = 0.794, p = 0.897$), and each data point was collected with 1000 samples of randomly chosen user pairs. Data analysis confirmed that the maximum time depth of 20 was never reached in any of the samples.

paths. Because of this hardness, we argued the necessity of developing practical path-finding heuristics. We introduced two paradigms for these heuristics based on when the purification operations are allowed to take place and discussed their trade-offs. Following this, we proposed a simplified noise model and developed a routing heuristic around a quantity called the *coherence probability* (the likelihood that a partially entangled pair will successfully teleport an unknown qubit). We then introduced our cost-vector formalism by making the observation that (under this simplified noise model), every partially entangled pair that could exist in the network may be characterised with a coherence probability and a *transmission probability*, which is the likelihood of the pair existing. We described how swapping operations relate to vertex contractions and explained how two concurrent edges may be combined into one using the Bennett purification protocol. With the cost-vector formalism established, we extended our model to accommodate scenarios in which routing takes place over time. Specifically, we showed how the use of a memory channel can be described as a swapping operation over a fictitious resource called a transitory pair. We discussed the implications of this and devised a basic ruleset to determine whether a path through a temporal network corresponds to a physically realisable routing protocol. We introduced the *temporal meta-graph*, which describes the entanglement and memory resources available to a network at various points in time, and we introduced *asynchronous nodes* which facilitate path-finding between end-users in the meta-graph. Following this, we devised two quantum routing algorithms that greedily purify the k shortest paths between one or more pairs of end users. Most notably, we showed that for highly congested networks, the performance of these routing algorithms did not substantially improve as more computers were added to the network. Rather, we found that increasing the time-depth available for routing was quite effective at unblocking the network.

ACKNOWLEDGEMENTS

We thank Darcy Morgan, Alexis Shaw, Marika Kieferova, Zixin Huang, Louis Tessler, Yuval Sanders, Jasminder Sidhu, Simon Devitt & Jon Dowling for a variety of insightful conversations. Deepesh Singh was supported by the Australian Research Council Centre of Excellence for Quantum Computation and Communication Technology (project CE110001027). Peter Rohde and Nathan Langford are funded by ARC Future Fellowships (projects FT160100397 and FT170100399, respectively).

Appendix A: Entanglement routing as Abelian groups

In developing our cost-vector formalism, we've simplified our network description in a way that allows our network operations (entanglement distribution, swapping and purification) to commute. Here, we formalise this observation with group-theoretic terms. If we assume that each channel in the network is partially dephasing or partially depolarising, then we find that the following algebraic rules hold. Take $F(f_1, f_2)$ to be the the fidelity after purification for two states with fidelity f_1, f_2 as given in Eq. 3.3 Then,

$$\begin{aligned} F(f_1, f_2) &= F(f_2, f_1), \\ F(F(f_1, f_2), f_3) &= F(f_1, F(f_2, f_3)), \\ F(f_1, 1/2) &= f_1, \\ F(f_1, 1 - f_1) &= \frac{1}{2}, \end{aligned} \tag{A1}$$

which, in the the domain of $[0, 1]$, allows purification to form an Abelian group. Furthermore, by considering the properties of the entanglement swapping operation $\mathcal{E}_{\text{swap}} := S$ defined in equation 2.7 we find that,

$$\begin{aligned} S(f_1, S(f_2, f_3)) &= S(S(f_1, f_2), f_3), \\ S(f_1, 1) &= f_1, \\ S(f_1, f_2) &= S(f_2, f_1), \\ S\left(f_1, \frac{2f_1 - 4}{2f_1 - 1}\right) &= 1, \end{aligned} \tag{A2}$$

which is an Abelian group under swapping in the domain $[0, 1] \setminus \frac{1}{2}$.

Now, considering success probability, we can define,

$$\begin{aligned} P(p_1, p_2) &= P(p_2, p_1), \\ P(P(p_1, p_2), p_3) &= P(p_1, P(p_2, p_3)), \\ P(p_1, 1) &= p_1, \end{aligned} \tag{A3}$$

This forms an Abelian monoid,

$$\begin{aligned} \hat{\rho}_1 * \hat{\rho}_2 &= \hat{\rho}_2 * \hat{\rho}_1, \\ (\hat{\rho}_1 * \hat{\rho}_2) * \hat{\rho}_3 &= \hat{\rho}_1 * (\hat{\rho}_2 * \hat{\rho}_3). \end{aligned} \tag{A4}$$

We stress that for arbitrary error models this relationship no longer holds. The Abelian nature of this result ultimately stems from the commutativity of the errors through the underlying processes, which need not hold in general.

Appendix B: Average L_1-distance between random user-pairs on a square lattice

The number of ways N, to pick two distinct vertices in an $n \times n$ grid lattice is equivalent to the number of ways to pick two distinct pairs of positive integers no greater than n:

$$N \equiv n^2(n^2 - 1) \tag{B1}$$

The average L_1 distance between two distinct vertices is therefore:

$$\langle L_1 \rangle = \frac{\sum_{x_1, x_2, y_1, y_2}^{n} |x_1 - x_2| + |y_1 - y_2|}{N} \tag{B2}$$

Where $(x_1, y_1), (x_2, y_2)$ are the coordinates of the vertices in the lattice. Expanding the series to separate x and y:

$$\langle L_1 \rangle = \frac{n^2(\sum_{x_1, x_2}^{n} |x_1 - x_2| + \sum_{y_1, y_2}^{n} |y_1 - y_2|)}{N} \tag{B3}$$

$$= \frac{n^2(2\Delta)}{N} \tag{B4}$$

Where

$$\Delta \equiv \sum_{x_1, x_2}^{n} |x_1 - x_2| = \sum_{y_1, y_2}^{n} |y_1 - y_2| \tag{B5}$$

Let $\Delta = \Delta^+ + \Delta^-$ where Δ^+ contains the terms such that $x_2 < x_1$, and Δ^- the ones where $x_1 < x_2$. By symmetry we see that, $\Delta^+ = \Delta^-$. Then,

$$\begin{aligned} \Delta = 2\Delta^+ &= 2 \sum_{x_1=1}^{n-1} \sum_{x_2=x_1+1}^{n} (x_2 - x_1) \\ &= \frac{n(n^2 - 1)}{3}. \end{aligned} \tag{B6}$$

By substitution, we find that

$$\langle L_1 \rangle = \frac{2}{3} n \tag{B7}$$

REFERENCES

Arab, Amir R (2021), "On diagonal quantum channels," Reports on Mathematical Physics **88** (1), 59–72.

Bennett, Charles H, Gilles Brassard, Claude Crépeau, Richard Jozsa, Asher Peres, and William K. Wootters (1993), "Teleporting an unknown quantum state via dual classical and einstein-podolsky-rosen channels," Physical Review Letters **70**, 1895.

Bennett, Charles H, Gilles Brassard, Sandu Popescu, Benjamin Schumacher, John A. Smolin, and William K. Wootters (1996a), "Purification of noisy entanglement and faithful teleportation via noisy channels," Physical Review Letters **76**, 722, arXiv:quant-ph/9511027.

Bennett, Charles H, David P. DiVincenzo, John A. Smolin, and William K. Wootters (1996b), "Mixed-state entanglement and quantum error correction," Physical Review A **54** (5), 3824–3851.

Chang, Alena, and Guoliang Xue (2022), "Order matters: On the impact of swapping order on an entanglement path in a quantum network," in *IEEE INFOCOM 2022 - IEEE Conference on Computer Communications Workshops (INFOCOM WKSHPS)*, pp. 1–6.

Coopmans, Tim, Robert Knegjens, Axel Dahlberg, David Maier, Loek Nijsten, Julio Oliveira, Martijn Papendrecht, Julian Rabbie, Filip Rozpędek, Matthew Skrzypczyk, Leon Wubben, Walter de Jong, Damian Podareanu, Ariana Torres Knoop, David Elkouss, and Stephanie Wehner (2020), "Netsquid, a discrete-event simulation platform for quantum networks," arXiv:2010.12535.

Dahlberg, Axel, and Stephanie Wehner (2018), "Simulaqron – a simulator for developing quantum internet software," Quantum Science & Technology **4**, 015001, arXiv:1712.08032.

Gilchrist, Alexei, Nathan K. Langford, and Michael A. Nielsen (2005), "Distance measures to compare real and ideal quantum processes," Phys. Rev. A **71**, 062310.

Goodenough, Kenneth, David Elkouss, and Stephanie Wehner (2021), "Optimizing repeater schemes for the quantum internet," Phys. Rev. A **103**, 032610.

Horodecki, Pawel, Michal Horodecki, and Ryszard Horodecki (1999), "General teleportation channel, singlet fraction and quasi-distillation," arXiv:quant-ph/9807091 [quant-ph].

Jiang, Liang, Jacob M. Taylor, Navin Khaneja, and Mikhail D. Lukin (2007), "Optimal approach to quantum communication using dynamic programming," Proceedings of the National Academy of Sciences **104** (44), 17291–17296.

Matsuo, Takaaki (2019), "Simulation of a dynamic, ruleset-based quantum network," arXiv:1908.10758 [quant-ph].

Pan, Jian-Wei, Dik Bouwmeester, Harald Weinfurter, and Anton Zeilinger (1998), "Experimental entanglement swapping: Entangling photons that never interacted," Physical Review Letters **80**, 3891.

Zajac, Sandra, and Sandra Huber (2021), "Objectives and methods in multi-objective routing problems: a survey and classification scheme," European Journal of Operational Research **290** (1), 1–25.